

## Supporting Information

### **Sonochemistry-assisted Photocontrolled Atom Transfer Radical Polymerization Enabled by Manganese Carbonyl**

Chen Wang<sup>1</sup>, Wenru Fan<sup>1\*</sup>, Zexuan Li<sup>1</sup>, Jiaqiang Xiong<sup>2</sup>, Wei Zhang<sup>2</sup>, Zhenhua Wang<sup>1\*</sup>

<sup>1</sup>Frontiers Science Center for Flexible Electronics & Xi'an Institute of Biomedical Materials and Engineering (IBME), Northwestern Polytechnical University, Xi'an 710072, China.

<sup>2</sup>Department of Obstetrics and Gynecology, Zhongnan Hospital of Wuhan University, Wuhan 430071, China.

# Table of Contents

<b>Figure S1.</b> Conversion analysis by $^1\text{H}$ NMR ( $\text{CDCl}_3$ ) of reaction mixture of SAP-ATRP of BA under the irradiation of single hood light, and the GPC traces. ....	4
<b>Figure S2.</b> Conversion analysis by $^1\text{H}$ NMR ( $\text{CDCl}_3$ ) of reaction mixture of SAP-ATRP of BA under ultrasound, and the GPC traces. ....	5
<b>Figure S3.</b> Conversion analysis by $^1\text{H}$ NMR ( $\text{CDCl}_3$ ) of reaction mixture of SAP-ATRP of BA under both the irradiation of hood light and ultrasound, and the GPC traces. ....	6
<b>Figure S4.</b> Conversion analysis by $^1\text{H}$ NMR ( $\text{CDCl}_3$ ) of reaction mixture of SAP-ATRP of BA with $DP_T = 200$ . ....	7
<b>Figure S5.</b> Conversion analysis by $^1\text{H}$ NMR ( $\text{CDCl}_3$ ) of reaction mixture of SAP-ATRP of BA with $DP_T = 300$ . ....	8
<b>Figure S6.</b> Conversion analysis by $^1\text{H}$ NMR ( $\text{CDCl}_3$ ) of reaction mixture of SAP-ATRP of BA with $DP_T = 400$ . ....	9
<b>Figure S7.</b> Conversion analysis by $^1\text{H}$ NMR ( $\text{CDCl}_3$ ) of reaction mixture of SAP-ATRP of BA with $DP_T = 800$ . ....	10
<b>Figure S9.</b> Conversion analysis by $^1\text{H}$ NMR ( $\text{CDCl}_3$ ) of reaction mixture of SAP-ATRP of MA under both the irradiation of hood light and ultrasound, and the GPC trace. ....	11
<b>Figure S10.</b> Conversion analysis by $^1\text{H}$ NMR ( $\text{CDCl}_3$ ) of reaction mixture of SAP-ATRP of EA under both the irradiation of hood light and ultrasound, and the GPC trace. ....	12
<b>Figure S11.</b> Conversion analysis by $^1\text{H}$ NMR ( $\text{CDCl}_3$ ) of reaction mixture of SAP-ATRP of MMA under both the irradiation of hood light and ultrasound, and the GPC trace. ....	13
<b>Figure S12.</b> Conversion analysis by $^1\text{H}$ NMR ( $\text{CDCl}_3$ ) of reaction mixture of SAP-ATRP of BMA under both the irradiation of hood light and ultrasound, and the GPC trace. ....	14
<b>Figure S13.</b> Conversion analysis by $^1\text{H}$ NMR ( $\text{CDCl}_3$ ) of reaction mixture of SAP-ATRP of BzMA under both the irradiation of hood light and ultrasound, and the GPC trace. ....	15
<b>Figure S14.</b> Conversion analysis by $^1\text{H}$ NMR ( $\text{D}_2\text{O}$ ) of reaction mixture of SAP-ATRP of SPMA under both the irradiation of hood light and ultrasound, and the GPC trace. ....	16
<b>Figure S15.</b> Conversion analysis by $^1\text{H}$ NMR ( $\text{CDCl}_3$ ) of PMA-Br. ....	17
<b>Figure S16.</b> Conversion analysis by $^1\text{H}$ NMR ( $\text{CDCl}_3$ ) of PMA- <i>b</i> -PEA-Br. ....	18
<b>Figure S17.</b> Conversion analysis by $^1\text{H}$ NMR ( $\text{CDCl}_3$ ) of <b>ON-OFF</b> , and the GPC traces. ..	19
<b>Figure S18.</b> Results for the effect of different contents of TPMA on polymerization. ....	20
<b>Figure S19.</b> Conversion analysis by $^1\text{H}$ NMR ( $\text{CDCl}_3$ ) of reaction mixture of SAP-ATRP of BA, and the GPC traces. $[\text{Cu}^{\text{II}}]_0 : [\text{TPMA}]_0 = 1:1$ . ....	21

<b>Figure S20.</b> Conversion analysis by $^1\text{H}$ NMR ( $\text{CDCl}_3$ ) of reaction mixture of SAP-ATRP of BA, and the GPC traces. $[\text{Cu}^{\text{II}}]_0: [\text{TPMA}]_0 = 1:4$ .	22
<b>Figure S21.</b> Conversion analysis by $^1\text{H}$ NMR ( $\text{CDCl}_3$ ) of reaction mixture of SAP-ATRP of BA, and the GPC traces. $[\text{Cu}^{\text{II}}]_0: [\text{TPMA}]_0 = 1:6$ .	23
<b>Table S1.</b> Results for polymerization of various monomers under concurrent stimuli in different solvents.	24
<b>Figure S22.</b> Conversion analysis by $^1\text{H}$ NMR ( $\text{CDCl}_3$ ) of reaction mixture of SAP-ATRP of MA in 50% v/v DMSO, and the GPC trace.	25
<b>Figure S23.</b> Conversion analysis by $^1\text{H}$ NMR ( $\text{CDCl}_3$ ) of reaction mixture of SAP-ATRP of MA in 50% v/v DMF, and the GPC trace.	26
<b>Figure S24.</b> Conversion analysis by $^1\text{H}$ NMR ( $\text{CDCl}_3$ ) of reaction mixture of SAP-ATRP of MA in 50% v/v anisole and the GPC trace.	27

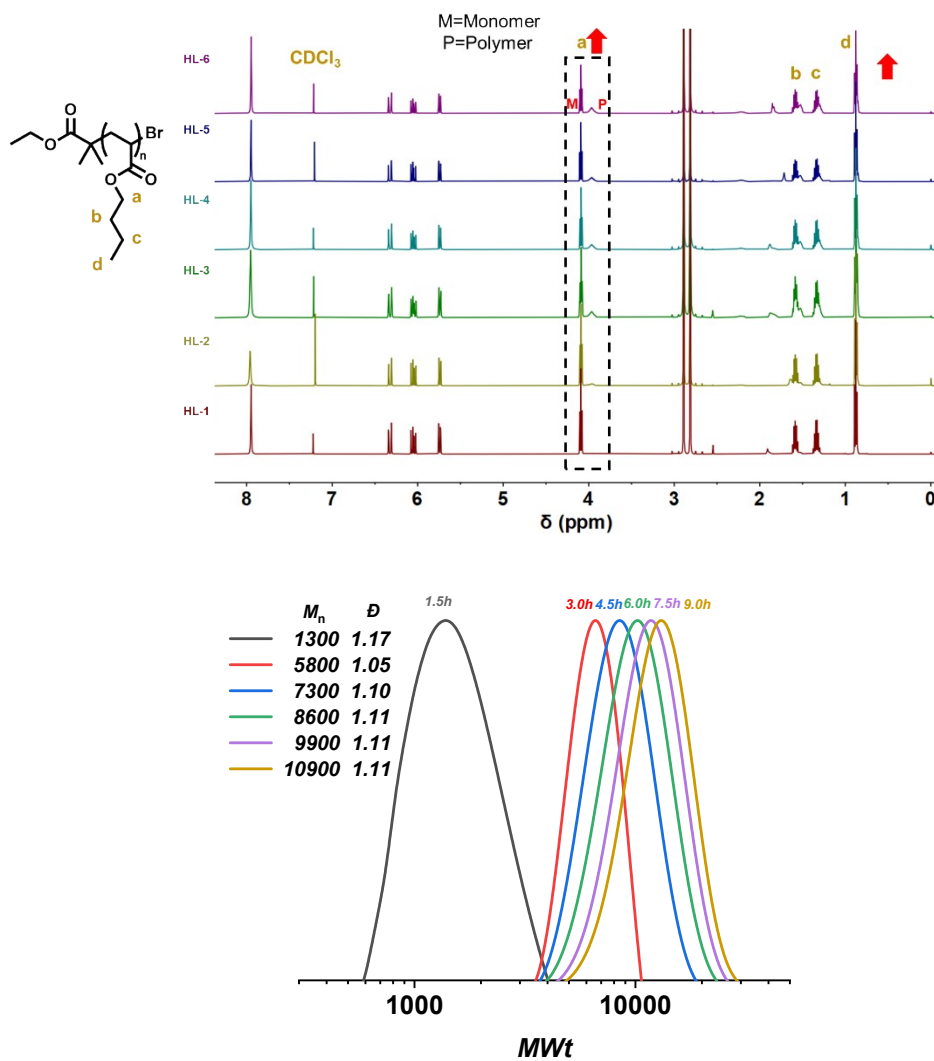


**Figure S1.** Conversion analysis by <sup>1</sup>H NMR (CDCl<sub>3</sub>) of reaction mixture of SAP-ATRP of BA under the irradiation of single hood light, and the GPC traces.

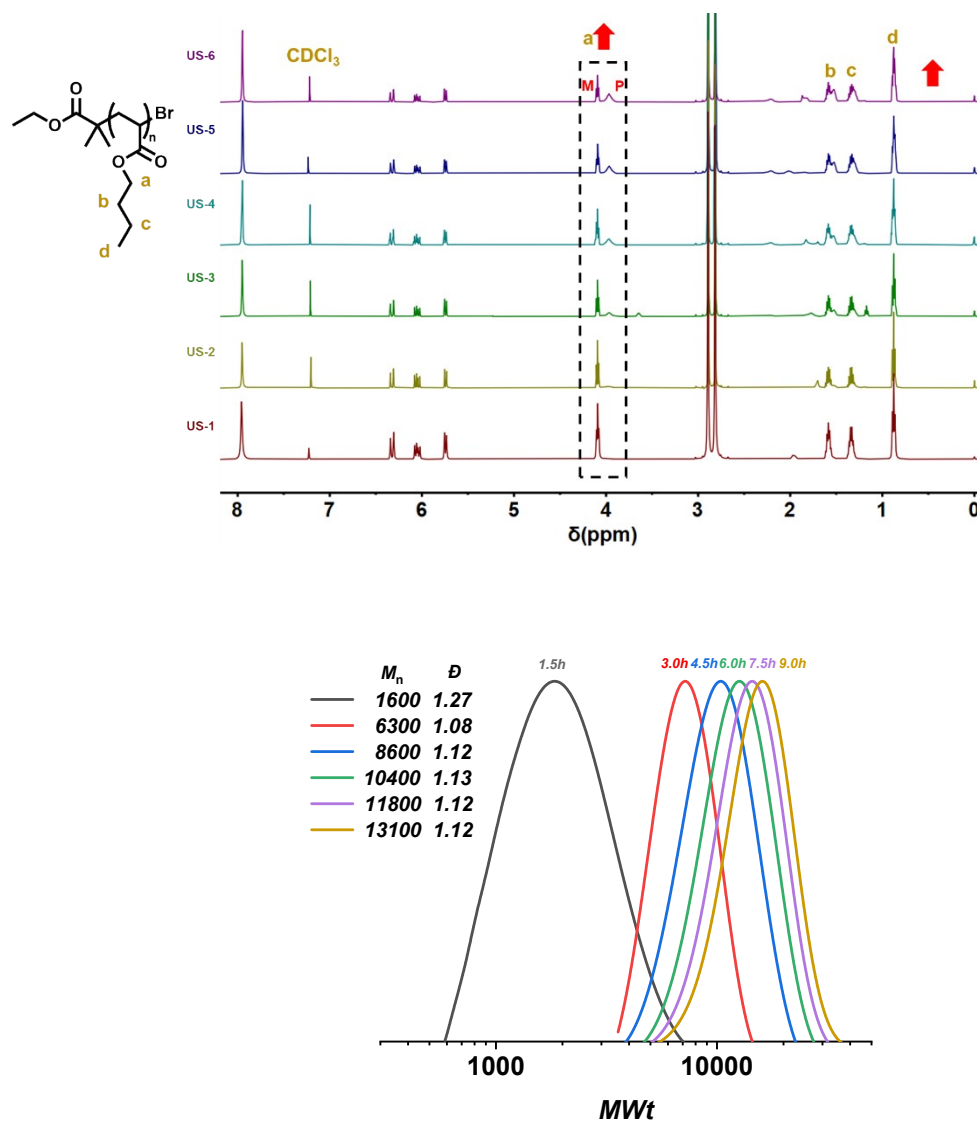


**Figure S2.** Conversion analysis by  $^1\text{H}$  NMR ( $\text{CDCl}_3$ ) of reaction mixture of SAP-ATRP of BA under ultrasound, and the GPC traces.

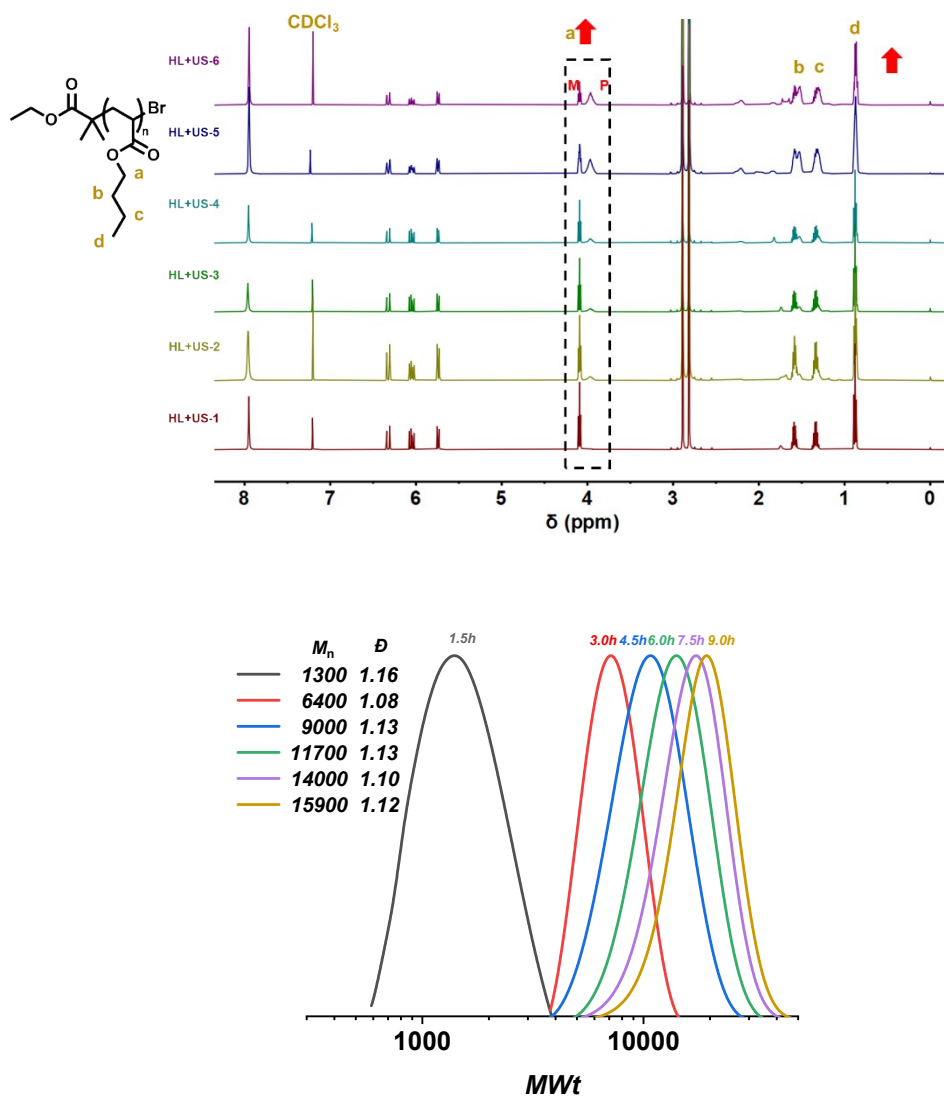


**Figure S3.** Conversion analysis by  $^1\text{H}$  NMR (CDCl<sub>3</sub>) of reaction mixture of SAP-ATRP of BA under both the irradiation of hood light and ultrasound, and the GPC traces.

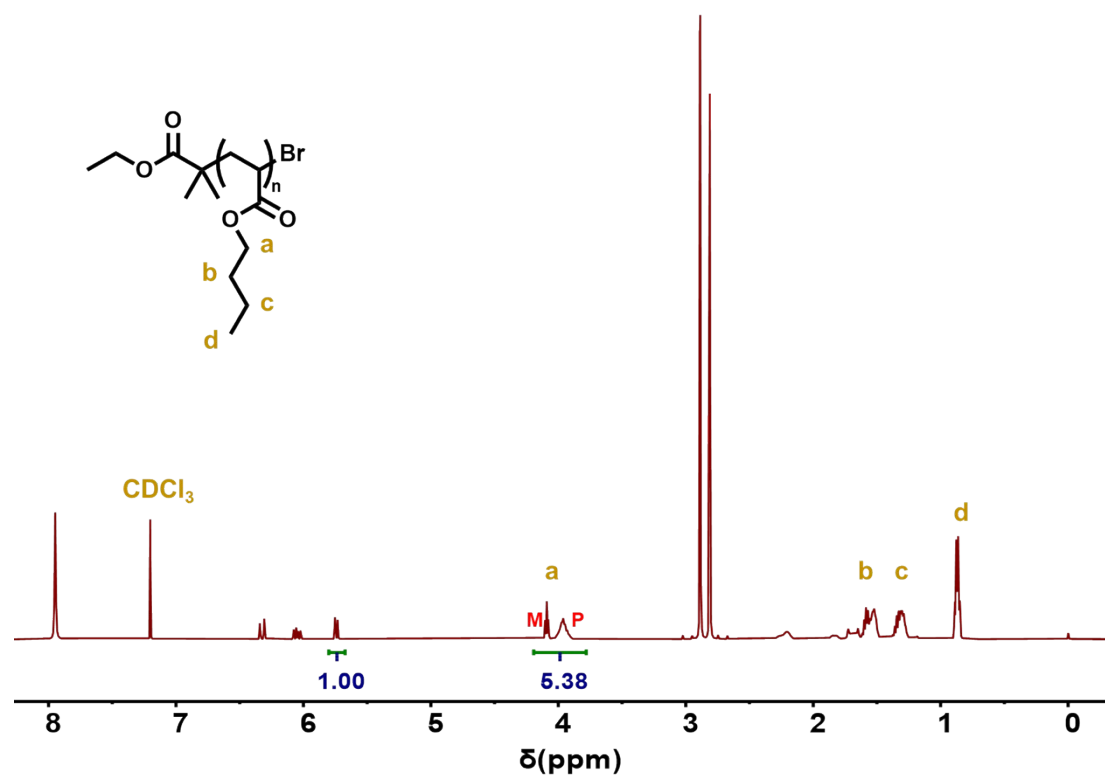


**Figure S4.** Conversion analysis by  $^1\text{H}$  NMR ( $\text{CDCl}_3$ ) of reaction mixture of SAP-ATRP of BA with  $DP_T = 200$ .

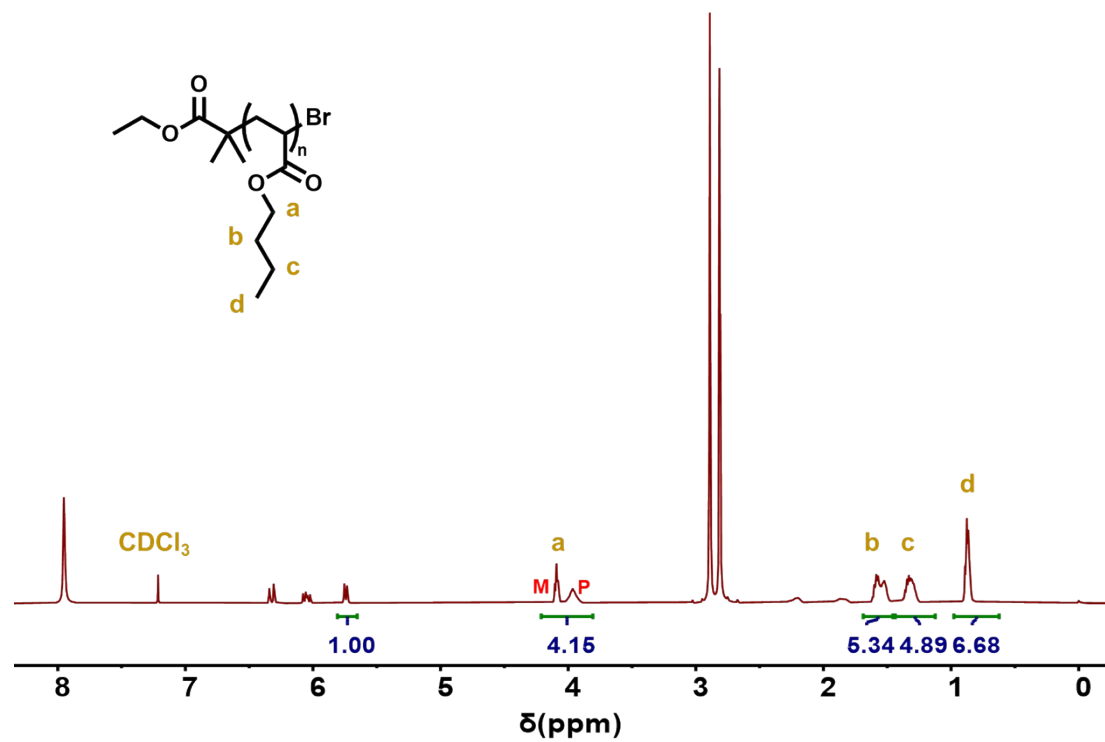


**Figure S5.** Conversion analysis by  $^1\text{H}$  NMR ( $\text{CDCl}_3$ ) of reaction mixture of SAP-ATRP of BA with  $DP_T = 300$ .



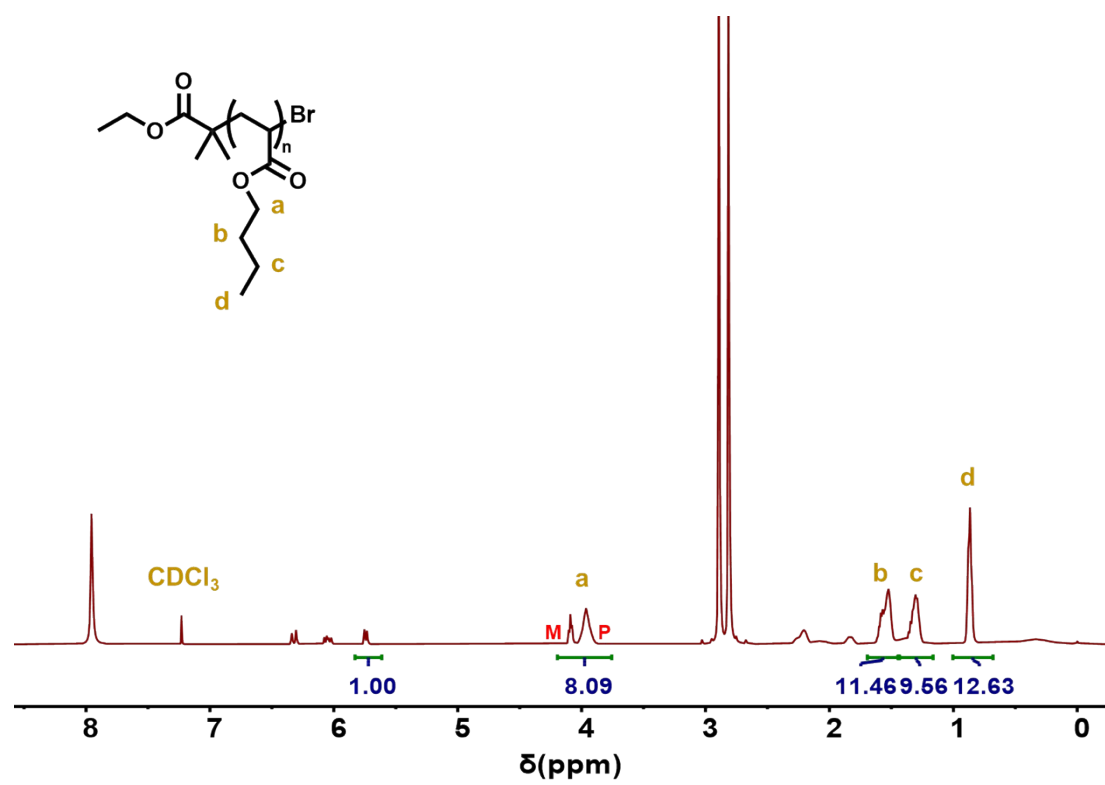


**Figure S6.** Conversion analysis by  $^1\text{H}$  NMR ( $\text{CDCl}_3$ ) of reaction mixture of SAP-ATRP of BA with  $DP_T = 400$ .

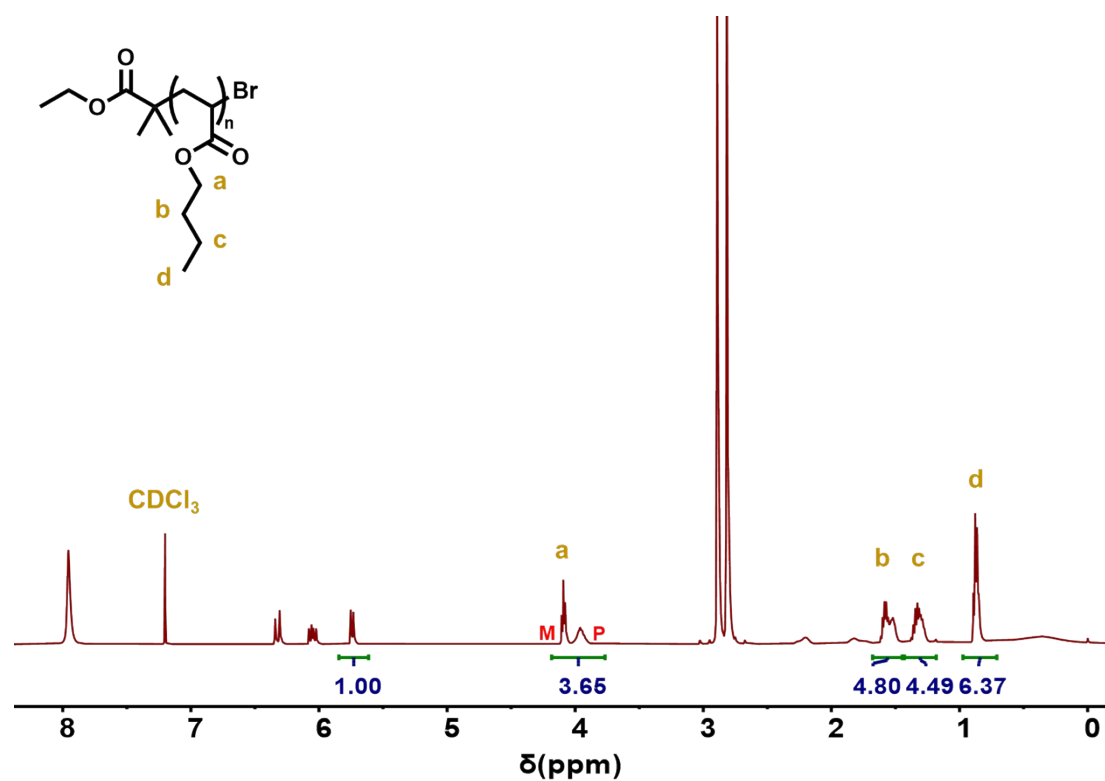


**Figure S7.** Conversion analysis by  $^1\text{H}$  NMR ( $\text{CDCl}_3$ ) of reaction mixture of SAP-ATRP of BA with  $DP_T = 800$ .

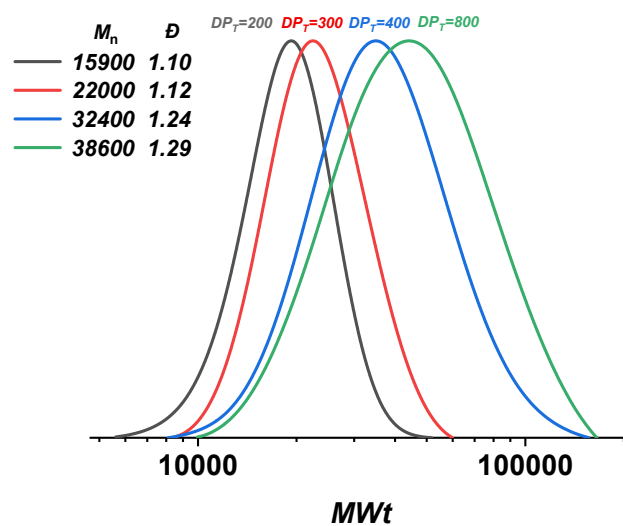


**Figure S8.** GPC traces of SAP-ATRP of BA with different  $DP_T$ .

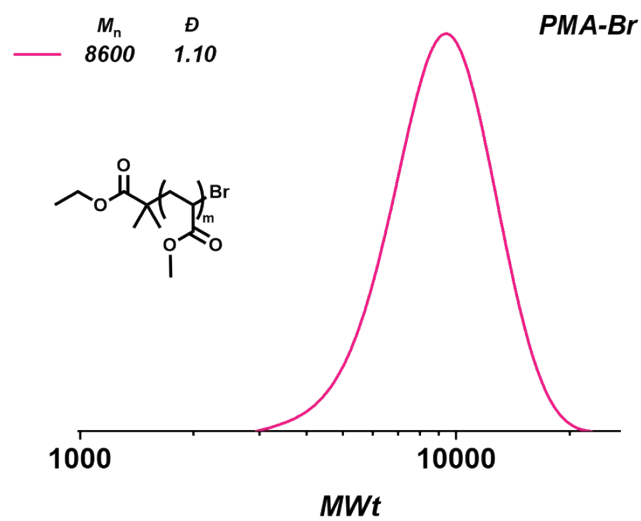
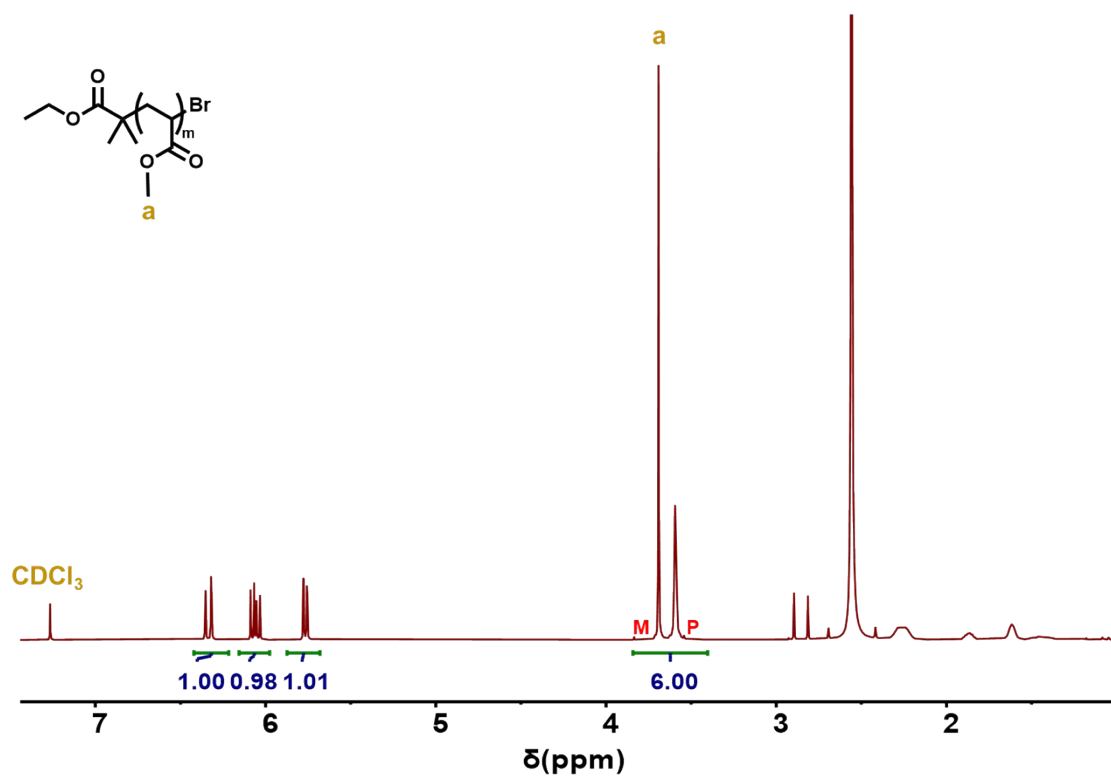


**Figure S9.** Conversion analysis by  $^1\text{H NMR}$  ( $\text{CDCl}_3$ ) of reaction mixture of SAP-ATRP of MA under both the irradiation of hood light and ultrasound, and the GPC trace.

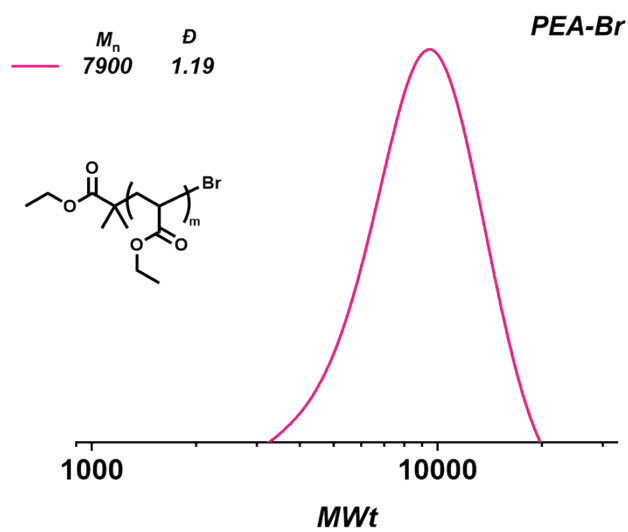
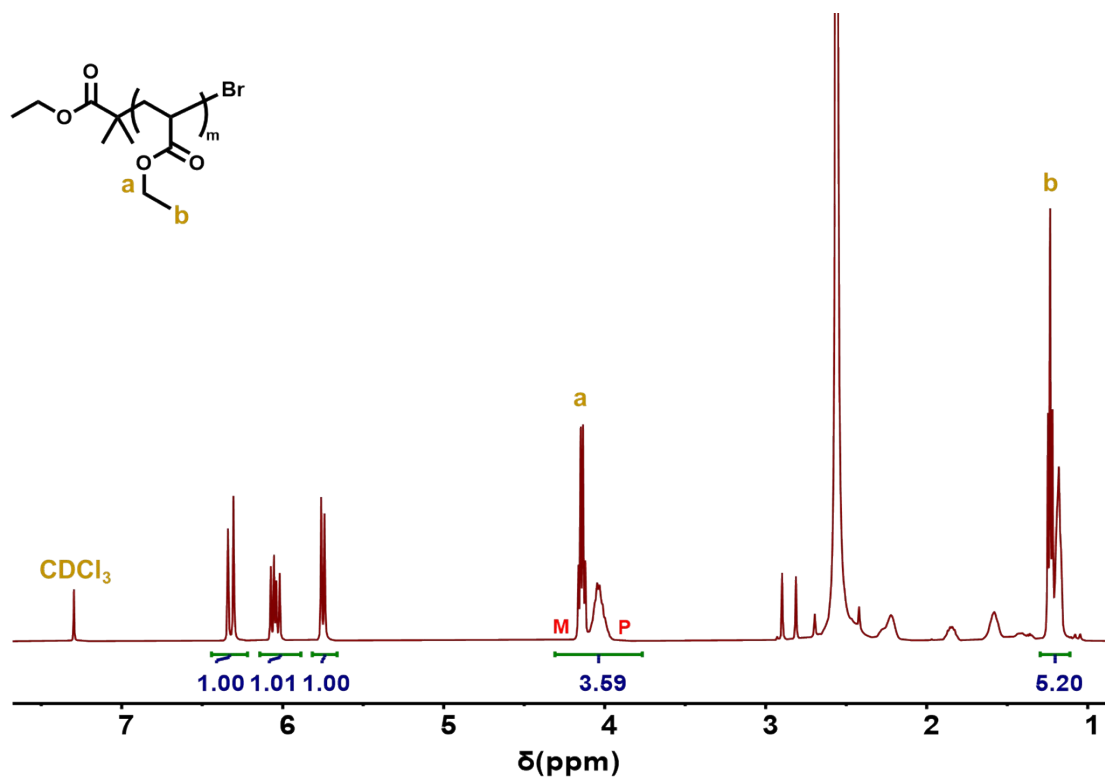


**Figure S10.** Conversion analysis by  $^1\text{H NMR}$  ( $\text{CDCl}_3$ ) of reaction mixture of SAP-ATRP of EA under both the irradiation of hood light and ultrasound, and the GPC trace.

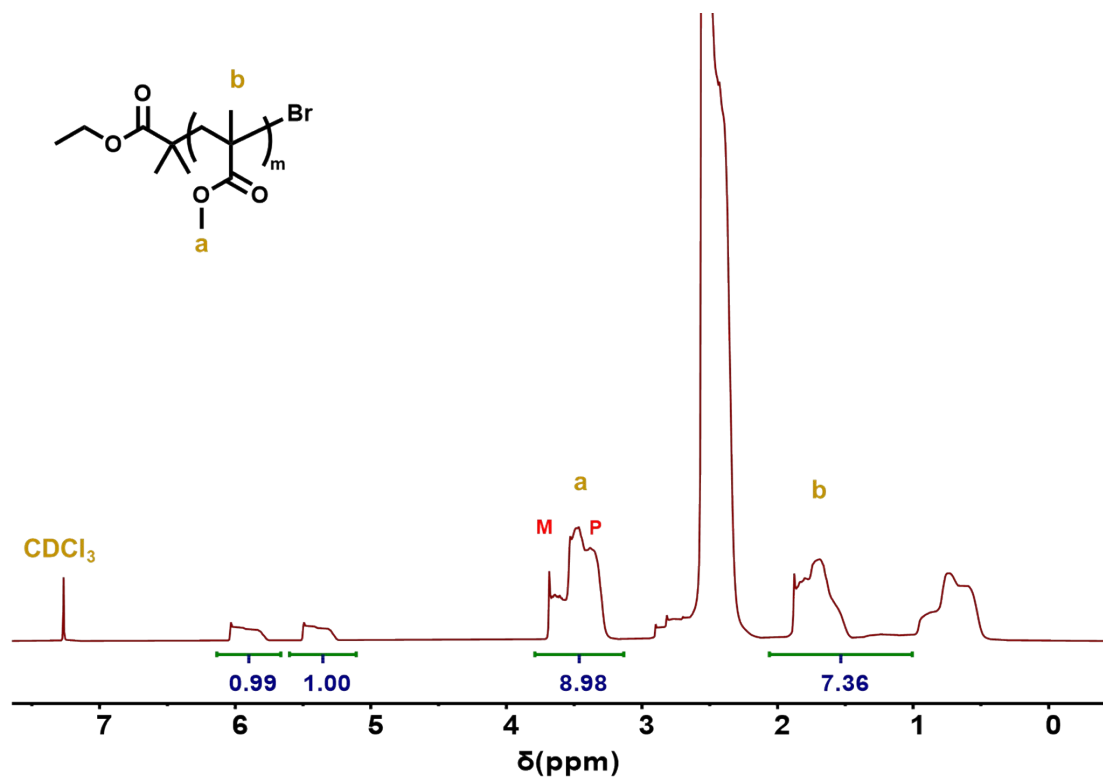
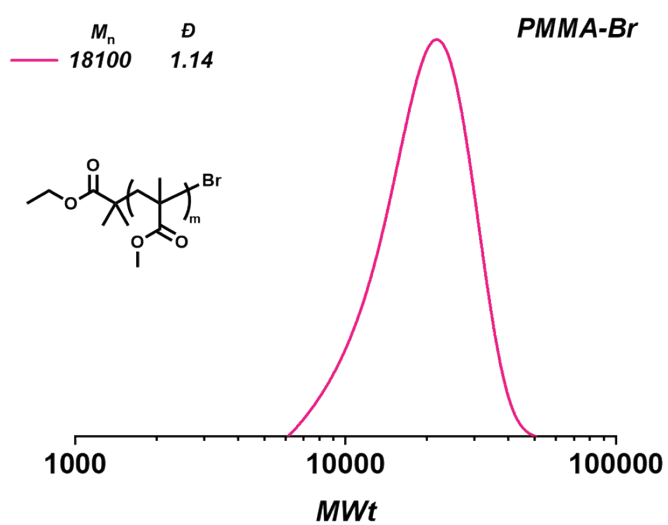


**Figure S11.** Conversion analysis by  $^1\text{H}$  NMR ( $\text{CDCl}_3$ ) of reaction mixture of SAP-ATRP of



MMA under both the irradiation of hood light and ultrasound, and the GPC trace.

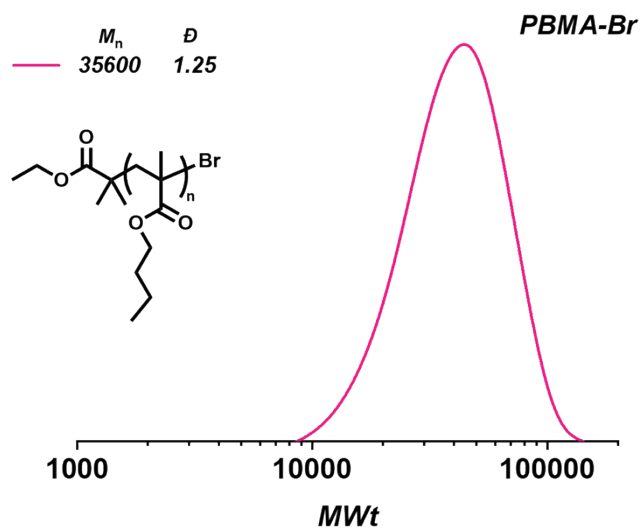
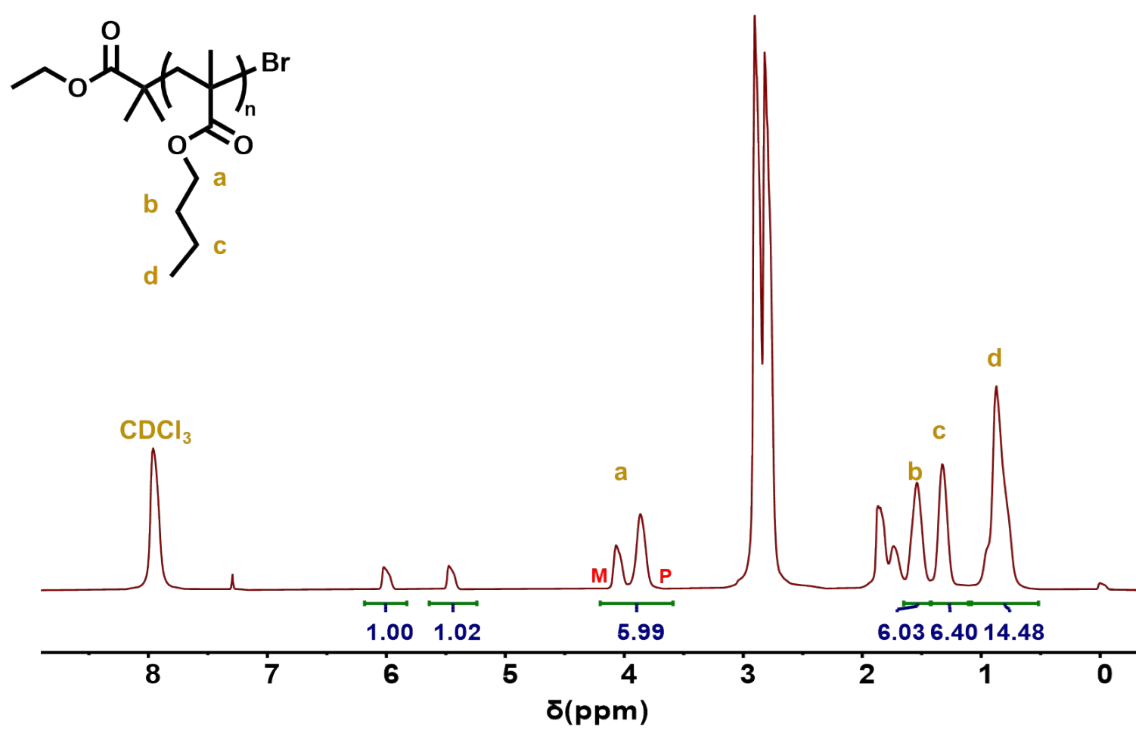


**Figure S12.** Conversion analysis by  $^1\text{H NMR}$  (CDCl<sub>3</sub>) of reaction mixture of SAP-ATRP of BMA under both the irradiation of hood light and ultrasound, and the GPC trace.

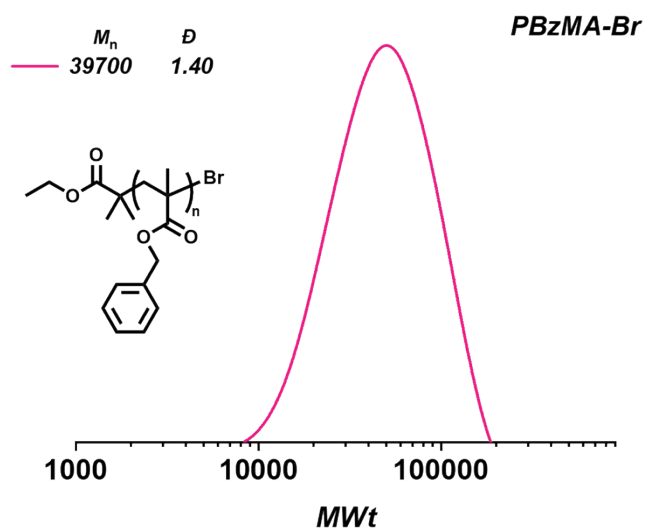
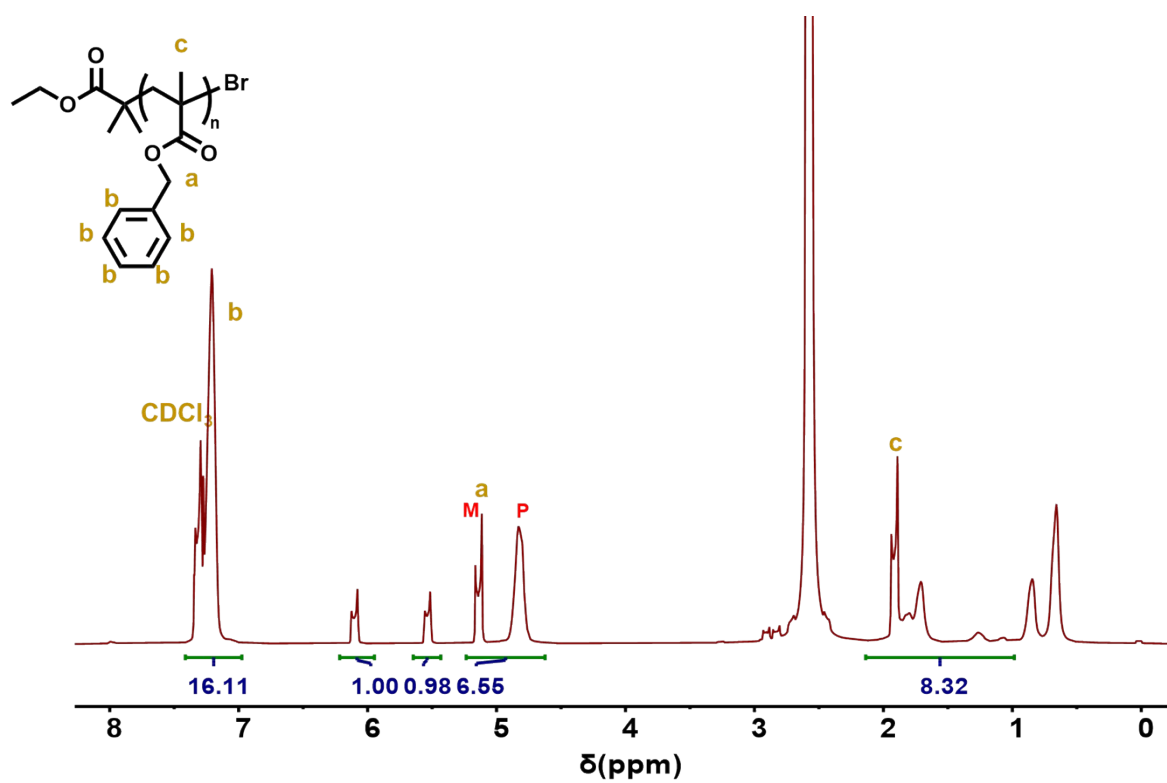


**Figure S13.** Conversion analysis by  $^1\text{H NMR}$  ( $\text{CDCl}_3$ ) of reaction mixture of SAP-ATRP of BzMA under both the irradiation of hood light and ultrasound, and the GPC trace.

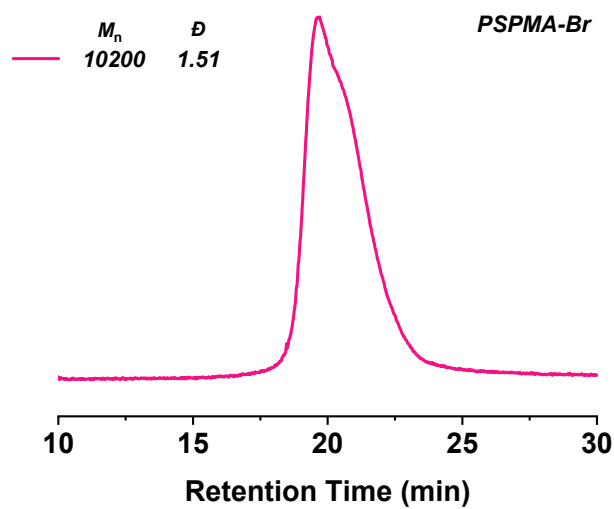
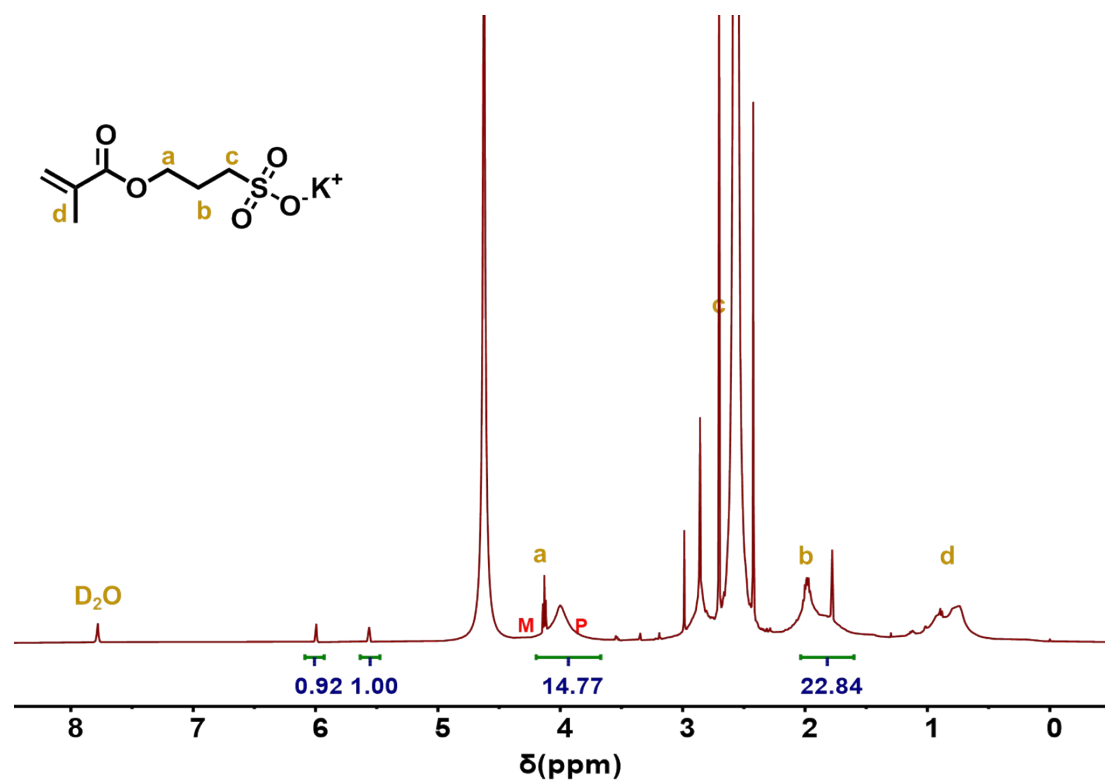


**Figure S14.** Conversion analysis by  $^1\text{H NMR}$  ( $\text{D}_2\text{O}$ ) of reaction mixture of SAP-ATRP of SPMA under both the irradiation of hood light and ultrasound, and the GPC trace.



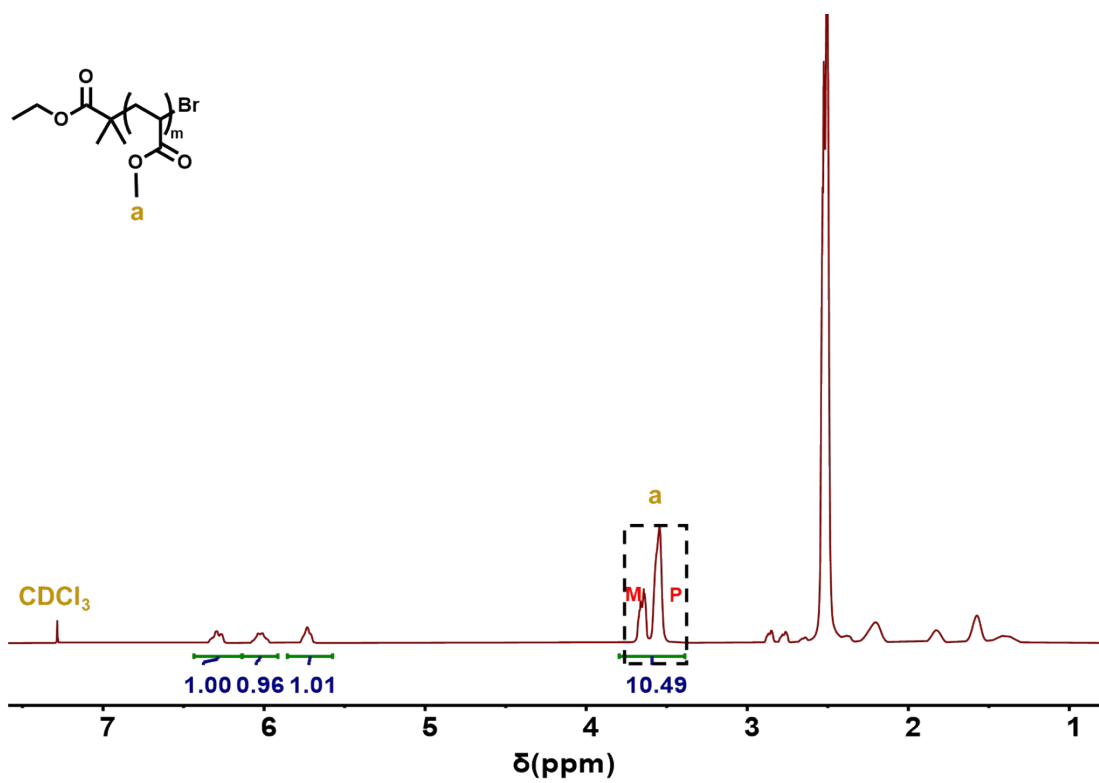


**Figure S15.** Conversion analysis by <sup>1</sup>H NMR (CDCl<sub>3</sub>) of PMA-Br.

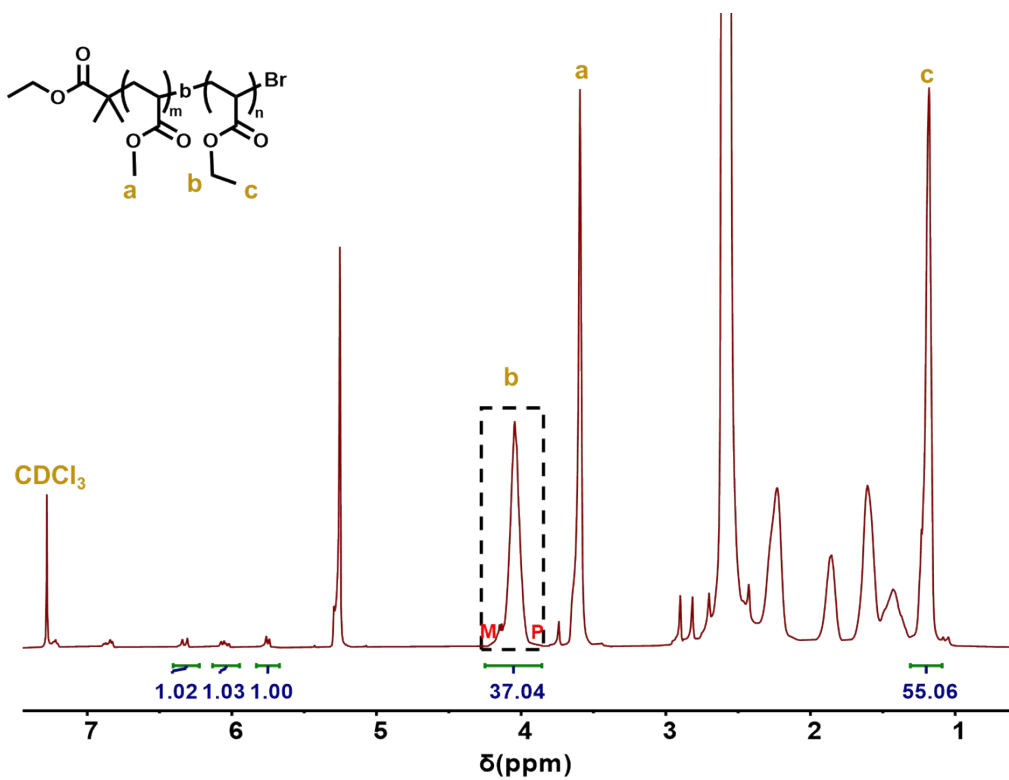


**Figure S16.** Conversion analysis by <sup>1</sup>H NMR (CDCl<sub>3</sub>) of PMA-*b*-PEA-Br.

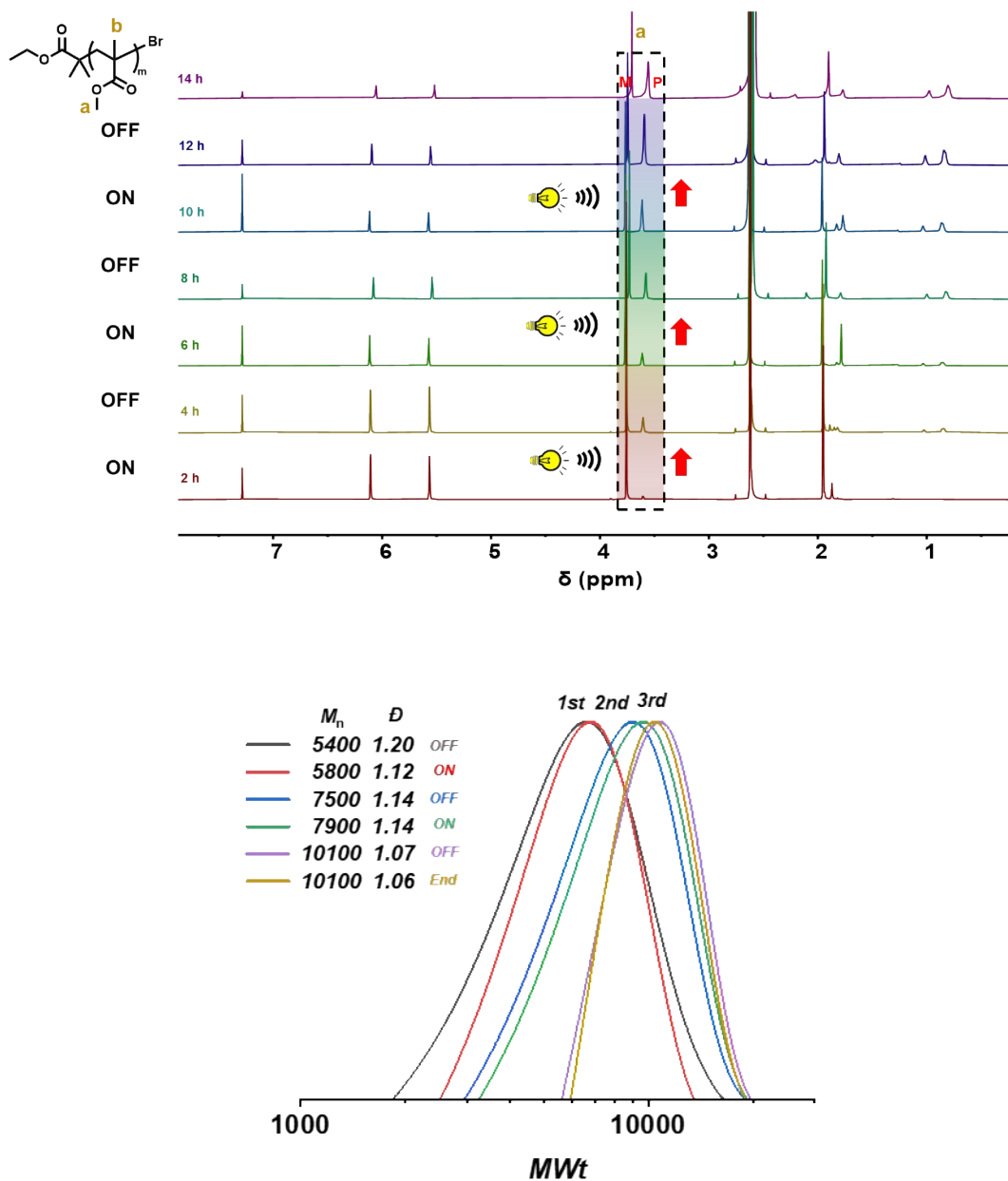
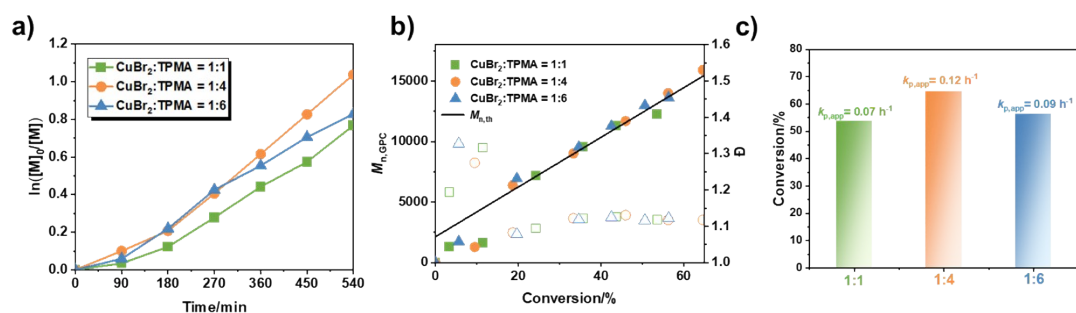
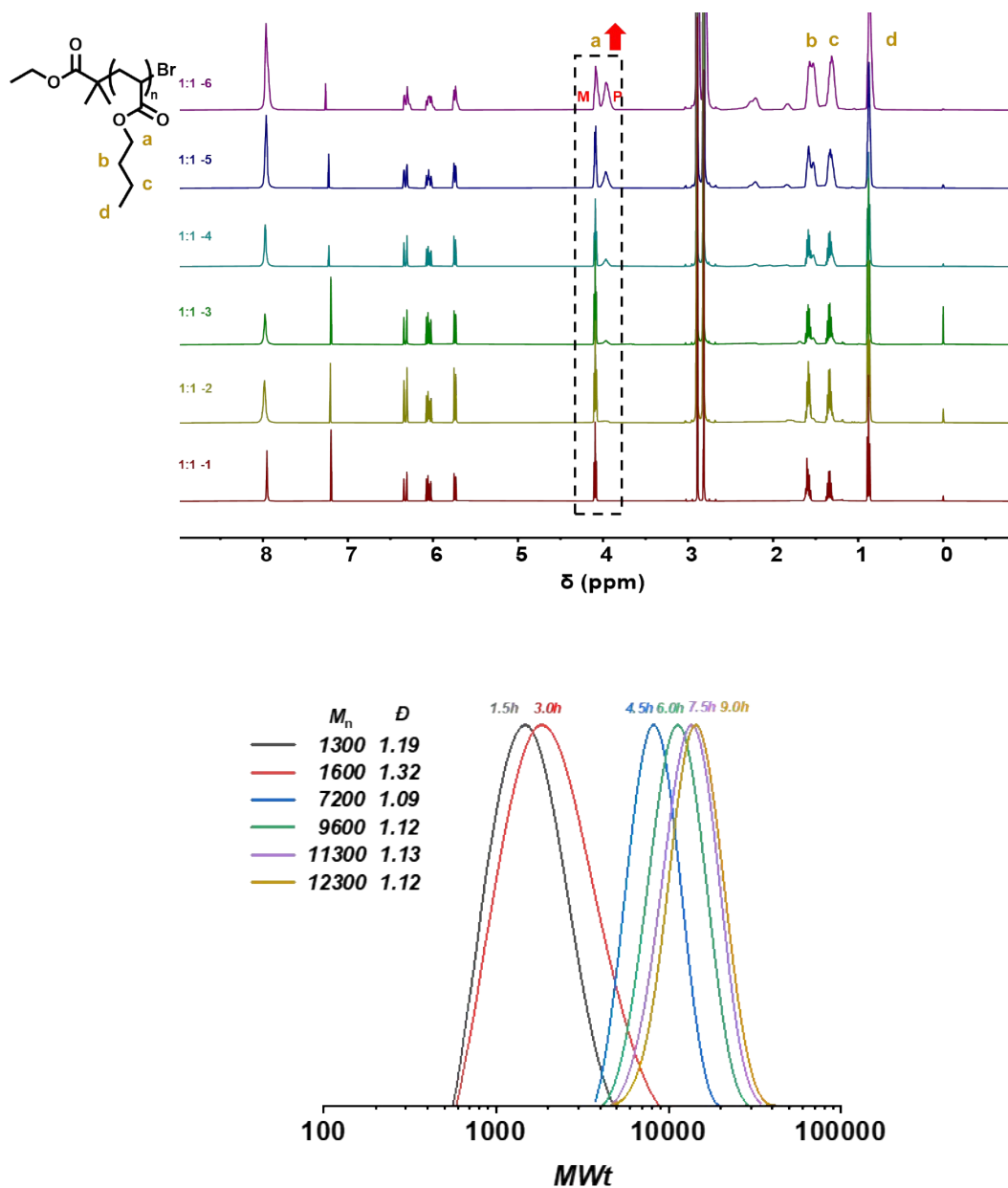


Figure S17. Conversion analysis by  $^1\text{H}$  NMR (CDCl<sub>3</sub>) of *ON-OFF*, and the GPC traces.



**Figure S18.** Results for the effect of different contents of TPMA on polymerization.  $[BA]_0 : [EBiB]_0 : [CuBr_2]_0 : [TPMA]_0 = 200:1:0.03:X$ , 0.45 wt %  $Mn_2(CO)_{10}$ , in 50% (v/v) DMF. (a) Semi-logarithmic kinetic plots evolution of polymerization under various stimuli. (b) Number-average molecular weight and molecular weight distribution ( $\bar{M}_w/\bar{M}_n$ ). (c) Conversion and apparent rate of the reaction.



**Figure S19.** Conversion analysis by  $^1\text{H}$  NMR (CDCl<sub>3</sub>) of reaction mixture of SAP-ATRP of BA, and the GPC traces.  $[\text{Cu}^{\text{II}}]_0: [\text{TPMA}]_0 = 1:1$ .

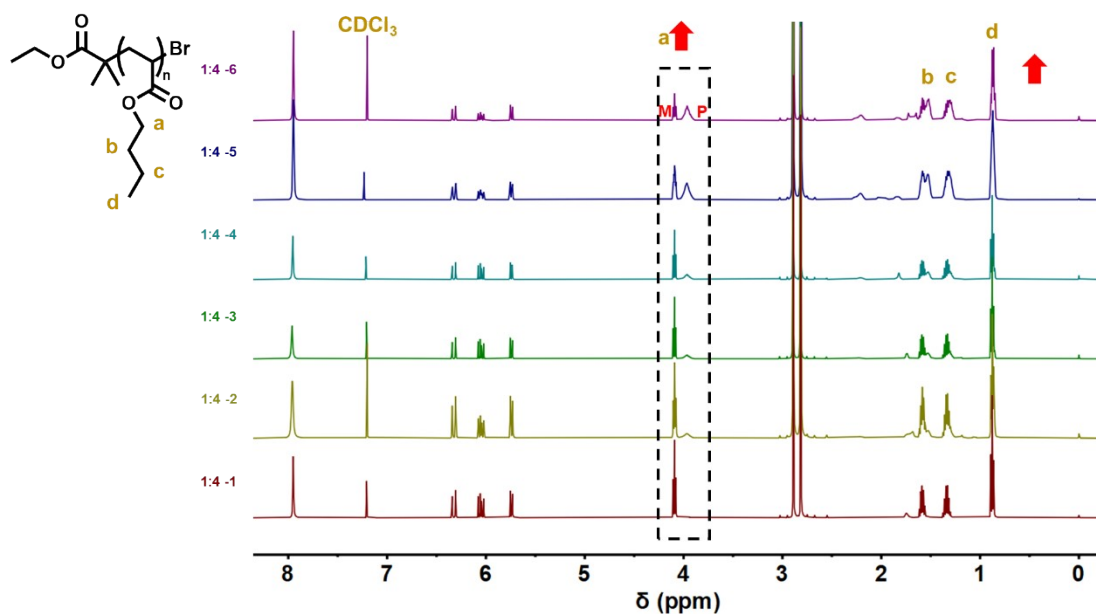
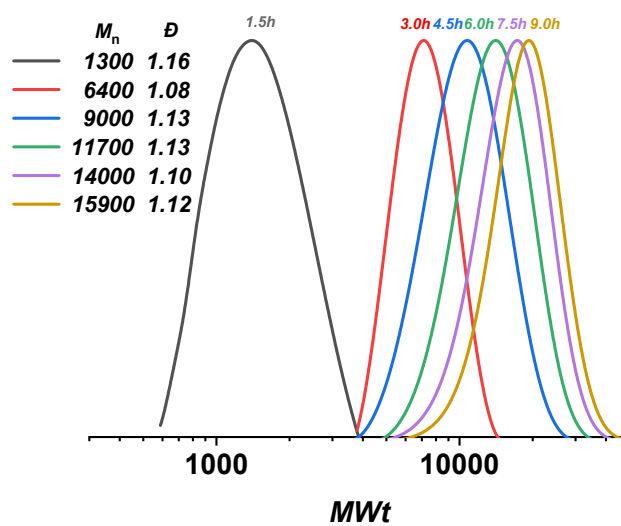


**Figure S20.** Conversion analysis by  $^1\text{H}$  NMR ( $\text{CDCl}_3$ ) of reaction mixture of SAP-ATRP of BA,



and the GPC traces.  $[\text{Cu}^{\text{II}}]_0: [\text{TPMA}]_0 = 1:4$ .

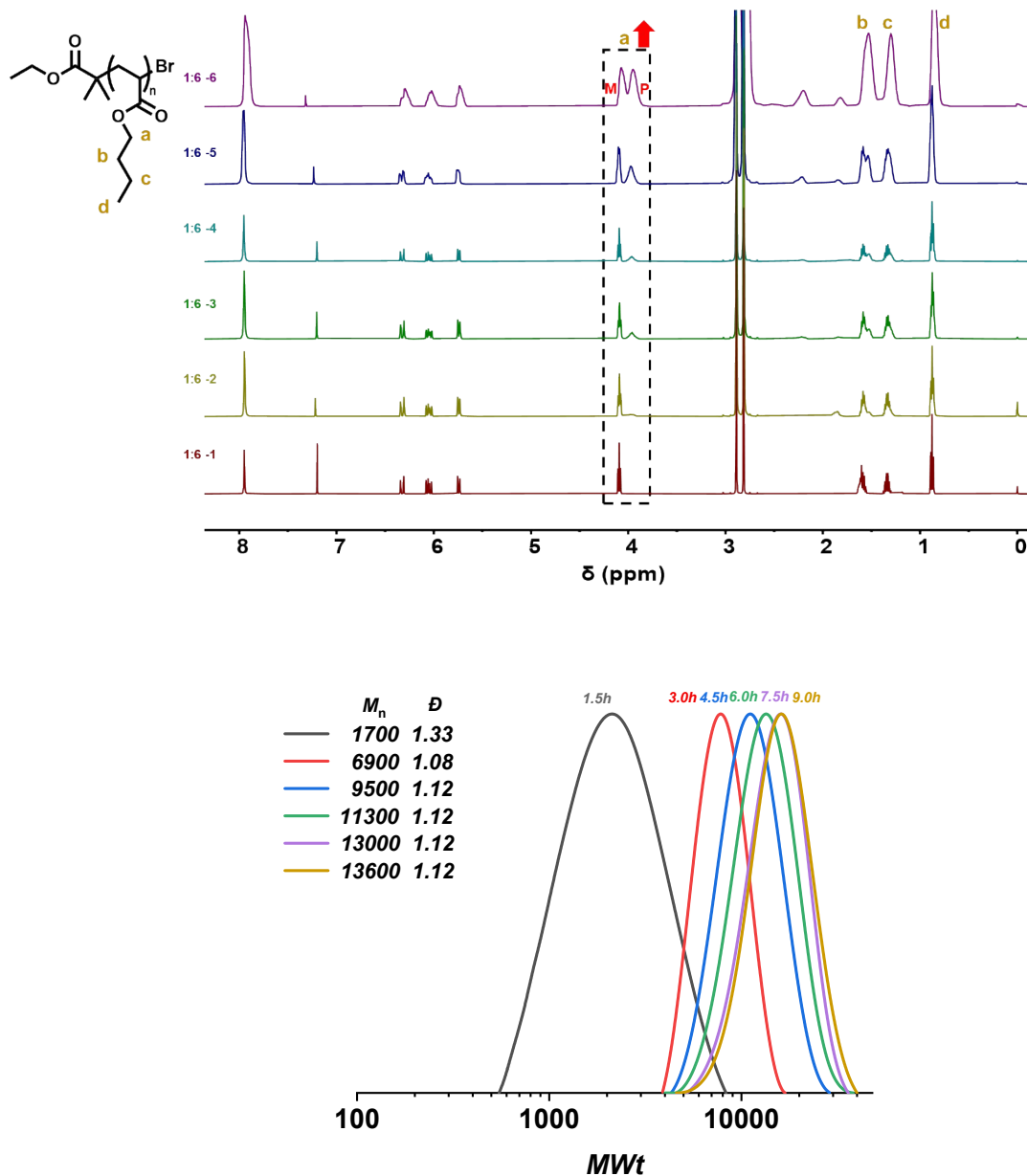


**Figure S21.** Conversion analysis by  $^1\text{H}$  NMR ( $\text{CDCl}_3$ ) of reaction mixture of SAP-ATRP of BA, and the GPC traces.  $[\text{Cu}^{\text{II}}]_0: [\text{TPMA}]_0 = 1:6$ .

**Table S1.** Results for polymerization of various monomers under concurrent stimuli in different solvents.

Entry <sup>a</sup>	Monomer	Solvent	T(h)	Conversion <sup>b</sup>	$M_{n,th}$ <sup>c</sup>	$M_{n,GPC}$ <sup>d</sup>	$\bar{D}$ <sup>d</sup>
1	MA	DMSO	5	50%	8800	8600	1.10
2	MA	DMF	5	50%	8800	8300	1.08
3	MA	Anisole	5	8%	1600	3700	2.73

<sup>a</sup> Reaction conditions:[MA]<sub>0</sub>:[EBiB]<sub>0</sub>:[CuBr<sub>2</sub>]<sub>0</sub>:[TPMA]<sub>0</sub>= 200:1:0.03:0.18 in 50% (v/v) DMSO/DMF/anisole, Magnetic stirring with a rod stirrer.<sup>b</sup> Conversion determined by <sup>1</sup>H NMR.<sup>c</sup> Calculated on the basis of conversion (i.e.,  $M_{n,th}=M_{EBiB}+[Monomer]_0/[EBiB]_0 \times conversion \times M_{monomer}$ ).<sup>d</sup> Determined by GPC in THF, based on linear PMMA as calibration standard.



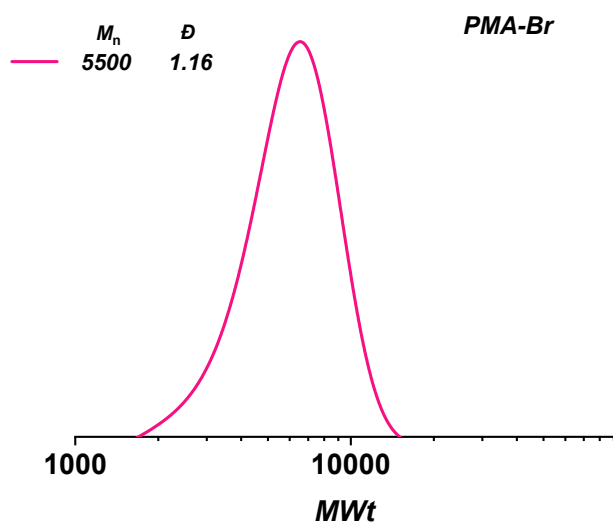
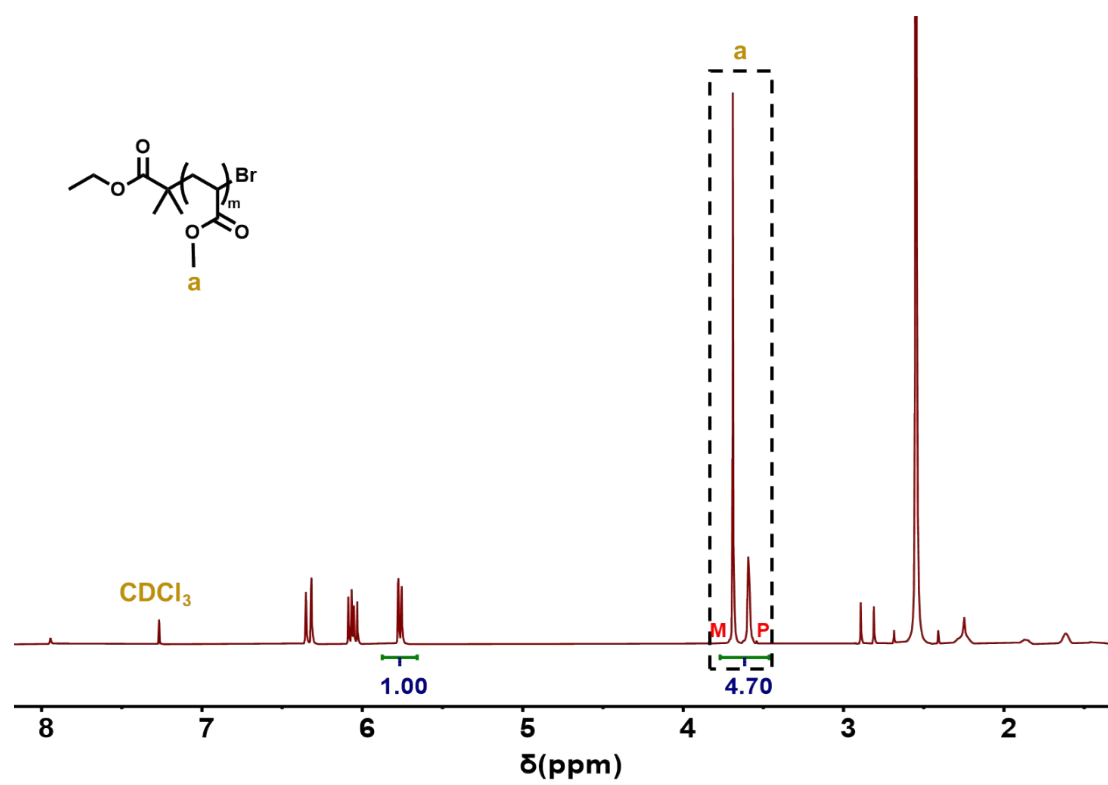


**Figure S22.** Conversion analysis by  $^1\text{H NMR}$  (CDCl<sub>3</sub>) of reaction mixture of SAP-ATRP of MA in 50% v/v DMSO, and the GPC trace.

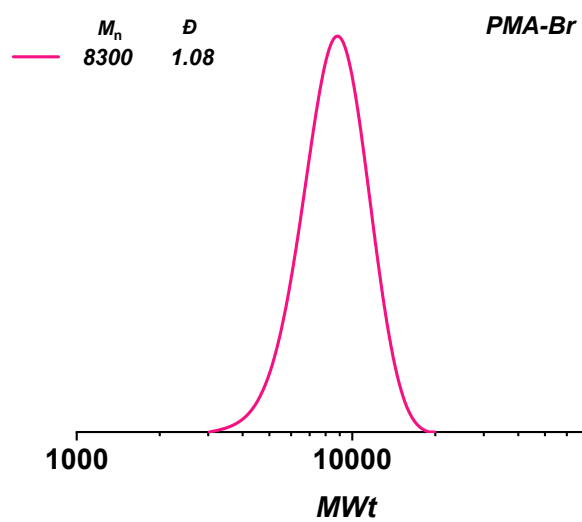
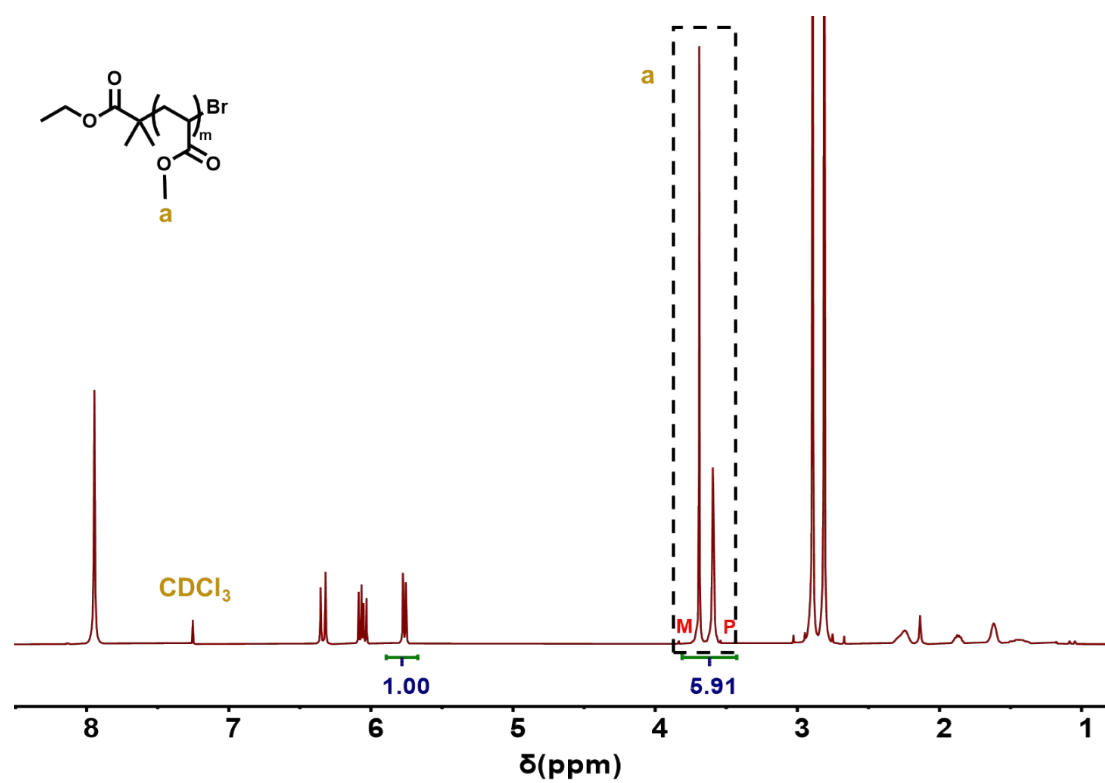


**Figure S23.** Conversion analysis by  $^1\text{H}$  NMR ( $\text{CDCl}_3$ ) of reaction mixture of SAP-ATRP of MA in 50% v/v DMF, and the GPC trace.

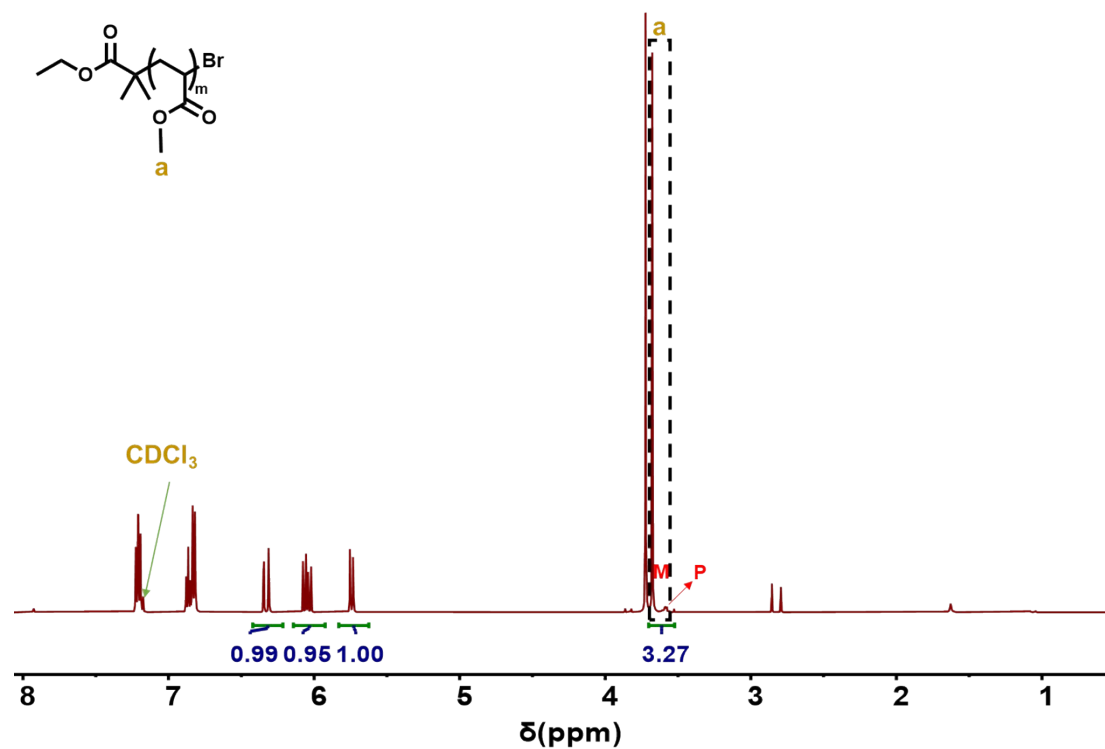
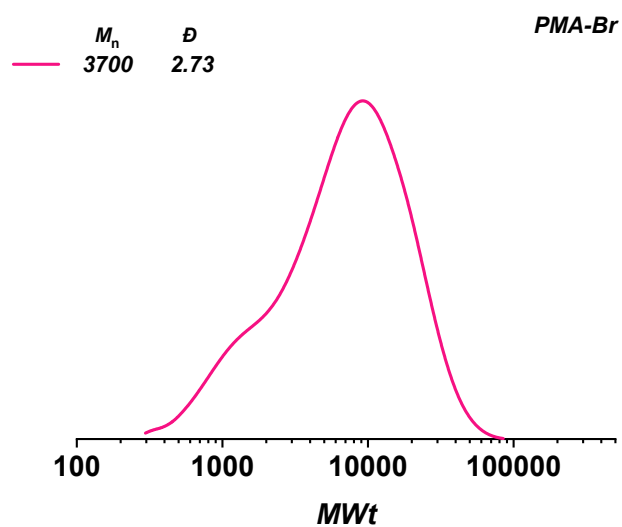


**Figure S24.** Conversion analysis by  $^1\text{H}$  NMR ( $\text{CDCl}_3$ ) of reaction mixture of SAP-ATRP of MA



in 50% v/v anisole and the GPC trace.

- 1) Xia, J.; Matyjaszewski, K. Controlled/"Living" Radical Polymerization. Atom Transfer Radical Polymerization Catalyzed by Copper(I) and Picolylamine Complexes. *Macromolecules* **1999**, *32*, 2434-2437.